Pergamon

Bioorganic & Medicinal Chemistry 9 (2001) 2243–2252

BIOORGANIC & MEDICINAL CHEMISTRY

Sequence Specific Recognition of ssDNA by a Lupus Autoantibody: Kinetics and Mechanism of Binding☆

Jennifer A. Beckingham[a] and Gary D. Glick[a,b,*]

[a]*Department of Chemistry, University of Michigan, Ann Arbor, MI 48109-1055, USA*
[b]*Department of Biological Chemistry, University of Michigan, Ann Arbor, MI 48109-1055, USA*

Received 12 January 2001; accepted 16 February 2001

Abstract—11F8 is a pathogenic anti-ssDNA monoclonal autoantibody isolated from a lupus-prone mouse. Previous studies have established that 11F8 is sequence specific. To determine the basis for the observed binding specificity, stopped-flow fluorescence spectroscopy was used to measure the kinetic parameters and establish the mechanisms for the association of 11F8 with its target sequence, noncognate, and nonspecific ssDNA ligands. The data revealed that sequence-specific binding follows a two-step mechanism where the initial association step is second order. Values of k_1 are fast and above the modified Smoluchowski limit for a diffusion limited interaction (10^5–$10^6\,M^{-1}\,s^{-1}$). The dependency of k_1 on [salt] and solvent polarity indicates that electrostatic steering is responsible for this rapid association rate. The second association step is rate limiting and is characteristic of an isomerization process during which binding interfaces are optimized. This step apparently is driven by the desolvation of hydrophobic surfaces within the binding interface. The differences in the rate of dissociation for the various DNA ligands suggest that specificity is governed primarily through the dissociation of the final complexes.

Introduction

Antibodies that bind DNA are a serological hallmark of the autoimmune disease systemic lupus erythematosus (SLE).[1,2] Deposition of anti-DNA/DNA complexes within kidney tissue leads to an inflammatory response that results in the organ damage (known as lupus nephritus) that can be fatal for some lupus patients.[3–5] In previous work, we generated a panel of anti-DNA hybridomas from a lupus-prone mouse.[6] One of these antibodies, 11F8, localizes kidney tissue through binding to DNA adherent to the glomerurlar basement membrane.[7] Previous work has shown that 11F8 occludes five bases upon binding DNA and displays a preference for oligo(T).[6] Subsequent binding-site selection experiments demonstrated that 11F8 is sequence specific, recognizing a -GYYTTC- epitope in the context of a stem-loop structure (Fig. 1).[8]

An extensive thermodynamic and structural analysis was carried out to ascertain the factors that govern sequence-specific, noncognate, and nonspecific ssDNA recognition by 11F8.[9] Sequence-specific binding is enthalpically driven, opposed by entropy, and is characterized by a negative change in heat capacity. A key factor in promoting sequence-specific and noncognate binding is an enthapically favorable release of water from the interacting surfaces. By contrast, nonspecific binding is entropically driven which is derived entirely by cation release from the nonspecific DNA ligand (i.e., the polyelectrolyte effect).[9]

The kinetic parameters of several sequence specific protein/nucleic acid interactions have been determined.[10–15] These studies, which have mostly been carried out on dsDNA binding proteins, have identified two main binding mechanisms. The first mechanism is a single-step bimolecular association,[14–18] whereas the second mechanism is a two-step process that includes a bimolecular association followed by a slow conformational change.[10,11,19,20] In the single-step binding mechanism, k_{on} can be slower than the modified Smoulouchski limit for diffusion controlled interactions (10^5–$10^6\,M^{-1}\,s^{-1}$) which suggests that recognition of various functional groups reduces the rate of binding.[14,16,21] In the two-step binding mechanisms, k_{on} is usually fast and is often greater then the predicted diffusion limit.[10,22] The second slower step generally involves small backbone and/or base/side chain movements within the binding interfaces that facilitate formation a high affinity complex.[23,24]

☆In honor of Peter Dervan on receipt of the Tetrahedron Prize

*Corresponding author. Tel.: +1-734-764-4548; fax: +1-734-615-8902; e-mail: gglick@umich.edu

0968-0896/01/$ - see front matter
PII: S0968-0896(01)00076-1

Within the DNA, conformational changes can be much larger, including strand melting and bending.[13,24]

Here, we describe experiments that probe the kinetics and mechanism of 11F8/ssDNA interactions. This research comprises part of our overall efforts to relate anti-DNA affinity and specificity with pathogenicity.[6–9] The results of which should assist in the development of new diagnostics and therapeutics for lupus. In addition, little is known about the kinetics of protein/ssDNA interactions.[11,19,25] Studying 11F8 should therefore also contribute to our overall understanding of the mechanisms by with proteins recognize ssDNA.

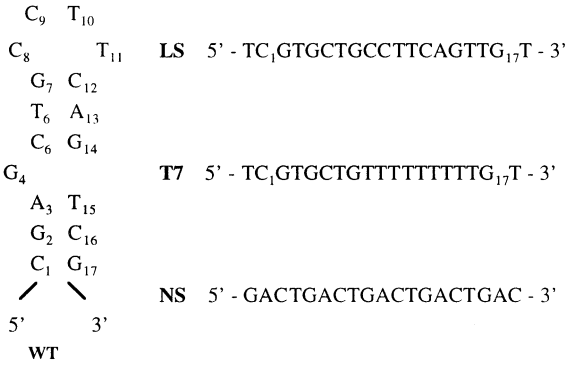

Figure 1. Sequence and secondary structure of the DNA ligands. **WT** is a 19-mer that adopts a hairpin conformation with a bulge base in position 4. This sequence is a truncated analogue of the 55-mer, identified through binding site selection experiments.[8] Truncation removes the PCR primers used in the selection process and does not cause any decrease in binding affinity. The base in position 4 was replaced with 2-aminopurine (2AP) to introduce a unique fluorescent label within the DNA structure. **LS** and **T7** are non-cognate 19-mers where positions 3 and 16 of **WT** were replaced with thymines to prevent formation of the stem-loop secondary structure. In **T7**, residues 8–14 were also replaced with thymine to remove both the structural and recognition elements of **WT**. **NS** is a nonspecific 19 mer, where each base is represented equally, and does not adopt any secondary structure.[9] Because 11F8 occludes ~5-bases on binding, both **T7** and **NS** contain multiple overlapping binding sites.

Results

Binding mechanism of the11F8/WT interaction

Upon interaction with ssDNA, the tryptophan fluorescence of 11F8 is decreased by ~30%.[6,9] This change provides a basis to measure the kinetic parameters of binding by stopped-flow spectroscopy. To determine the rate of association for each DNA sequence, an excess of DNA was mixed with 11F8 (1:1 v/v). Because the initial signal changes observed on binding were rapid, occurring within the deadtime of the instrument, sucrose was added (up to 40% w/v) to increase the viscosity of the buffer and decrease the rate of association. The reaction curve for the interaction between **WT** and 11F8 was biphasic, with an initial quench in tryptophan fluorescence ($k_{obs} = 35\,s^{-1}$) that was followed by a second slower quench in fluorescence emission ($k_{obs} = 4.2\,s^{-1}$; Fig. 2). The amplitude of the first step is 20% of the entire signal change. The rate of this initial varied linearly with [**WT**], typical of a simple bimolecular association process (Table 1). The rate of the second phase was independent of [**WT**], indicating that this step is rate limited by a different process than a simple binding interaction. The K_d measured from the first phase, using the relationship k_{-1}/k_1 is ~2000-fold higher than that measured at equilibrium. This finding suggests that the first signal change is due to the formation of an encounter complex and that the subsequent slow signal change represents a process leading to the formation of the high affinity complex (Scheme 1).

The kinetic data for binding **WT** could also be described by an alternative model that involves the isomerization of either 11F8 or **WT** into an active form, as a prerequisite for binding (Scheme 2). This model has been proposed for protein/protein binding mechanisms where one protein can exist in more than one conformation at equilibrium, although only one conformation is active.[26–28]

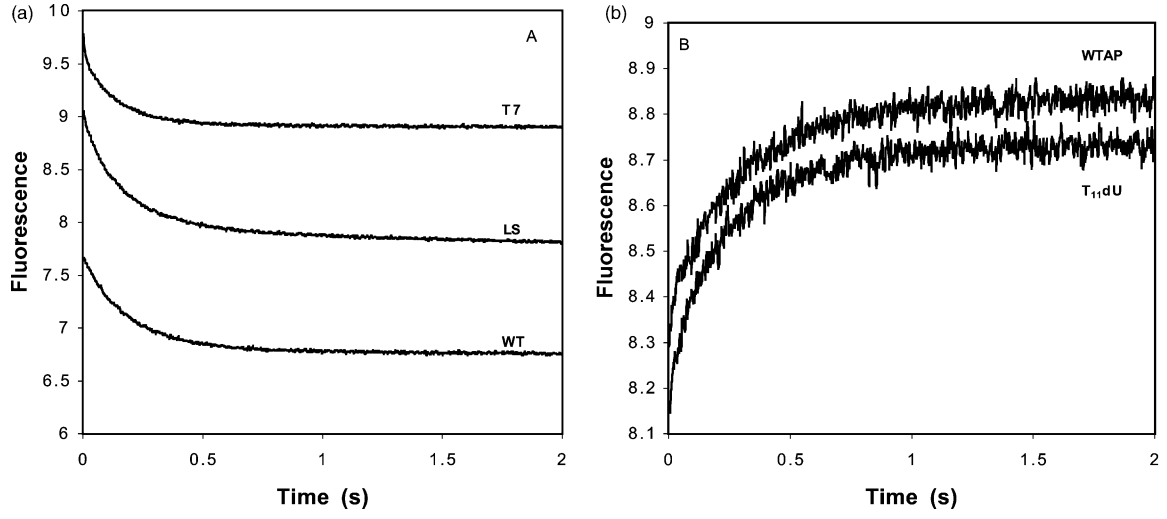

Figure 2. Association traces for each of the ssDNA sequences with 11F8. (A) Reaction traces for the interaction between 11F8 (100 nM) with **WT**, **LS** and **T7** (2 μM). The excitation wavelength was set at 280 nm to monitor changes in tryptophan emission. (B) Association of **WTAP** (2 μM) and $T_{11}dU$ with 11F8 (100 nM), monitoring the interaction through 2AP fluorescence. The excitation wavelength was set at 310 nm to monitor changes of 2AP emission.

Table 1. Kinetic parameters for the association and dissociation of **WT** with 11F8

DNA	k_1 ($\mu M^{-1} s^{-1}$)	k_{-1} (s^{-1})	k_2 (s^{-1})	k_{-2} (s^{-1})	$K_{d(enc)}$ (μM)	$K_{d(eq)}$ (nM)
WT	13.6±1.3	9.04±2.0	4.2±0.3	0.00334±0.0002	0.66±0.1	0.41±0.1
WTAP	9.21±0.89	6.18±1.3	4.3±0.2	0.00231±0.0001	0.67±0.1	0.43±0.1
WTAP[a]	10.3±0.66	7.21±0.8	4.4±0.3	0.00426±0.0002	0.70±0.1	0.52±0.1

[a][11F8] > > [**WT**].

Under the experimental conditions described above, the results suggest that 11F8 exists in the two conformations, 'active' (11F8) and 'inactive' (11F8*). The active 11F8 would be bound immediately upon mixing with excess **WT** (k_1), causing a shift in the 11F8/11F8* equilibrium. In this scheme, the second slow change in fluorescence would represent the rate-limiting isomerization of the inactive protein to the active form, which then binds to **WT** (k_2). If the conformational change causes no change in tryptophan emission, from the comparison of the amplitudes of the different steps, we can predict that at equilibrium, 20% of 11F8 exists in the active form.

These two mechanisms can be distinguished by measuring the kinetics of binding with 11F8 in excess of **WT**. Under these conditions, the mechanism shown in Scheme 2 predicts that there would be a sufficient [11F8] in the active form to bind to the smaller amount of DNA, and thus would decrease the amplitude of k_2 if not eliminate it altogether. However, if the mechanism in Scheme 1 is correct, no significant change in any of the rate constants would be expected. As seen in Table 1, our data are most consistent with Scheme 1. Such two-step binding mechanisms, where an initial encounter complex is formed followed by a conformational change, have been proposed for many biological systems, including protein/protein,[29–31] protein/nucleic acid,[10,11,19] protein/ligand,[32,33] and antigen/antibody complexes.[34,35] The encounter complex is thought to be very similar to the final complex, but with a reduced contact area.[36] The second slow step increases the number of interactions, thereby increasing the contact area between the two surfaces, to form a high-affinity complex.

$$11F8 + DNA \underset{k_{-1}}{\overset{k_1}{\rightleftharpoons}} (11F8{\bullet}DNA)^* \underset{k_{-2}}{\overset{k_2}{\rightleftharpoons}} 11F8{\bullet}DNA$$

Scheme 1. k_1 and k_{-1} represent the forward and reverse rate constants for the formation of the encounter complex (11F8/DNA)* and k_2 describes the rate limiting step of association and k_{-2} is the reverse of this step.

$$11F8 \underset{k_{-1}}{\overset{k_1}{\rightleftharpoons}} 11F8^* + DNA \underset{k_{-2}}{\overset{k_2}{\rightleftharpoons}} 11F8{\bullet}DNA$$

Scheme 2.

The dissociation kinetics of the 11F8/**WT** complex was determined by displacement because the affinity for **WT** is too high for dilution to cause enough dissociation to be measured using fluorescence spectroscopy. The introduction of a unique fluorescent group (2AP), which had little effect on the affinity of the complex compared to **WT** (Table 1), enabled the dissociation rates to be measured. The **WTAP** sequence was complexed to 11F8 and then mixed with an excess of **WT**. The fluorescence of the 2AP was monitored as the **WTAP** dissociated from the 11F8. If the dissociation of the complex is limited by the reversal of k_2 as indicated by Scheme 1, then k_{-2} can be estimated from eq (1).

$$K_{d(eq)} = (k_{-1}.k_{-2})/(k_1.k_2) \quad (1)$$

where $K_{d(eq)}$ is the dissociation constant measured at equilibrium. For the interaction between **WTAP** and 11F8, $k_{-2} = 0.0026\ s^{-1}$.

The kinetic trace for the dissociation of 11F8/**WTAP** was biphasic, yielding rates of 0.1 and $0.003\ s^{-1}$, where the amplitude of the initial step was $< 5\%$ of the entire signal change (Fig. 4). The dissociation rates were independent of [**WT**]. The rate of the initial signal change yielded a result significantly slower than $6.18\ s^{-1}$ which is an estimate based on the y-intercept of the plot k_{obs} versus [DNA] as explained in methods (Table 1). This finding can be explained by comparing the relative amplitude of the different steps. In the association process, the formation of the **WTAP** encounter complex only accounts for 20% of the total fluorescence change (Fig. 3). As the encounter and final complexes existing at equilibrium will dissociate simultaneously upon mixing with **WT**, the largest proportion of the signal change will be due to k_{-2}, partly masking the smaller signal change represented by k_{-1}. The net effect of this process will be to apparently 'slow down' k_{-1}.[37] The rate of the second slower step is $0.003\ s^{-1}$, similar to the value for k_{-2}, of $0.0026\ s^{-1}$ predicted from eq (1).

Mechanisms of LS, T7, T11dU and NS binding to 11F8

Binding experiments were conducted with the non-cognate ligands, **LS**, **T7** and $T_{11}dU$ to elucidate the kinetic basis of sequence specificity. Each sequence formed an initial encounter complex that was followed by a slower rate-limiting step (Table 2, Figs. 2 and 3). Since the introduction of the 2AP to the G_4 position does not result in a fluorescence change upon binding to **LS** or **T7**, an alternative method was designed to study the dissociation of these complexes. These experiments

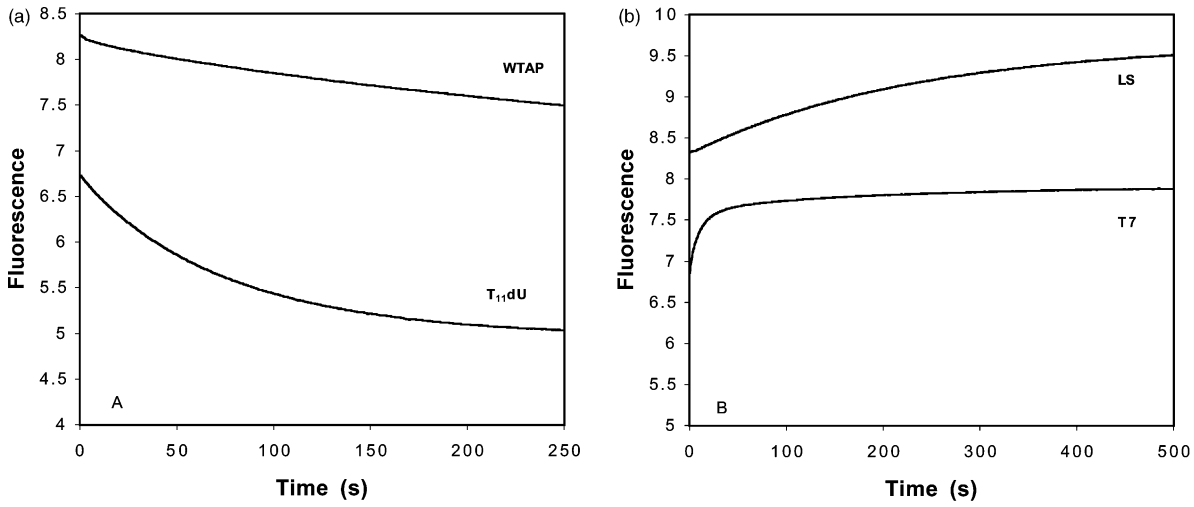

Figure 3. Dissociation of the 11F8/DNA complexes. (A) Traces of the 11F8/**WTAP** and 11F8/T_{11}dU complexes. The pre-formed complexes were mixed with an excess of **WT** which binds rapidly to the newly dissociated 11F8. The signal change observed is the change in 2AP as the **WTAP** and T_{11}dU dissociates from 11F8. (B) Dissociation of **LS** and **T7** from 11F8 was measured by mixing pre-formed complexes with **WTAP**. When excited at 310 nm, the fluorescence signal observed is the association of **WTAP** with the newly dissociated 11F8, which is rate limited by the dissociation of **LS** and **T7**. The second slow change in fluorescence of 11F8/**T7** dissociation trace results from photodegradation.

involved mixing an excess of **WTAP** with the requisite complexes. Although **WTAP** binds to 11F8 quickly in non-competitive conditions, the rate of association here is limited to the rate of dissociation of the complex (k_{-2}). If the dissociation of the 11F8/**LS** and 11F8/**T7** complexes were rate limited by the reversal of k_2, then the rate of this 'association' (11F8 + **WTAP**) would be slower than either of the two association steps measured for the formation of the complex in the absence of **LS** or **T7** (Table 2). An initial fast change in fluorescence corresponding to k_{-1} was not detected in the dissociation traces of either the 11F8/**LS** or 11F8/**T7** complexes indicating that a sufficiently small population of the encounter complex was present.

The results measured for the association and dissociation of each sequence with 11F8 are shown in Table 2 and are consistent with Scheme 1. A comparison of the affinity of the 11F8/**WT** and 11F8/T_{11}dU complexes show that there is a 6-fold decrease in the affinity of the latter at equilibrium. The kinetic parameters indicate that this phenomenon is mediated entirely through changes in k_{-2}, indicating that the methyl group of T_{11} is important for the final stability of the 11F8/**WT** complex.

Upon complexation with 11F8, the completely non-specific sequence, **NS**, quenched the tryptophan fluorescence by 30%. The reaction traces are very similar in appearance to those observed with **WT**, **LS** and **T7**, with an initial fast decrease in emission followed by a slow decrease. The slower quench in emission is more complex requiring multi-exponential analysis, giving at least two values that are not easily distinguishable. This situation probably reflects the presence of overlapping binding sites, present within the **NS** sequence. Consequently no further data was collected for the formation of the 11F8/**NS** complex.

Temperature dependence of binding

The Arrhenius plot of the 11F8/**WTAP** interaction is shown in Figure 4 and the corresponding energetic parameters are presented in Table 3. From the activation energies it can be seen that the temperature coefficients of the two association steps are different as expected from two different processes. The energy barrier to be surmounted for the second step of association is lower than that required for the dissociation of the encounter complex making it the more energetically

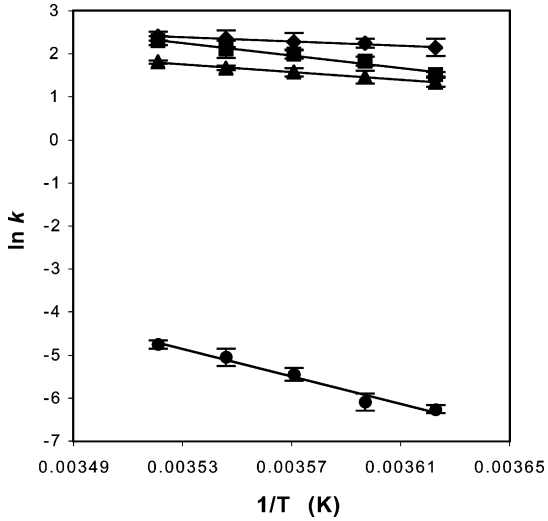

Figure 4. Arrhenius plots for k_1(◆), k_{-1} (■), k_2 (▲) and k_{-2}(●) for each step of the 11F8/**WT** interaction. The combination of the small signal change of k_{obs} for step 1 and low signal-to-noise ratio resulting from sucrose in the binding buffer, meant that temperature dependence of binding could only be monitored over a small temperature range (3–11 °C). The viscosity of the buffers containing sucrose are highly dependent on temperature, therefore, values of k_1 and k_{-1} were corrected to the viscosity observed for 10% w/v sucrose at 5 °C as explained in methods.

Table 2. Kinetic parameters for the association and dissociation of noncognate and nonspecific sequences with 11F8

Sequence	k_1 ($\mu M^{-1} s^{-1}$)	k_{-1} (s^{-1})	k_2 (s^{-1})	k_{-2} (s^{-1})	$K_{d(enc)}$ (μM)	$K_{d(eq)}$ (nM)
$T_{11}dU$	10.7±0.71	6.9±0.4	4.3±0.1	0.0152±0.001	0.65±0.1	2.4±0.2
LS	15.1±1.2	10.2±2.0	4.2±0.1	0.0354±0.001	0.68±0.1	5.2±0.2
T7[a]	61.0±4.4	36.2±4.2	3.7±0.2	0.371±0.05	0.594±0.03	4.9±0.5
NS[b]	32.2±3.1	43.4±5.2	ND[c]	ND	1.3±0.2	88±7

[a]20 mM Tris–HCl, 150 mM NaCl, 20% w/v sucrose, pH 8.0.
[b]20 mM Tris–HCl, 50 mM NaCl, 40% w/v sucrose, pH 8.0.
[c]ND, not determined.

favorable pathway for the encounter complex. The values of $\Delta H^{\ddagger}$ for each step, calculated from the Eyring equation are positive as expected for the formation and disruption of bonds occurring in each step of the interaction.[38] The $\Delta S^{\ddagger}$ for the initial association step is unfavorable, representing loss of rotational, translational and vibrational degree of freedom, typical of bimolecular association processes.[38] $\Delta S^{\ddagger}$ is smaller, although still unfavorable, in the second step indicating further loss in the freedom of individual side chains are contributing to this additional unfavorable entropy. As expected, $\Delta S^{\ddagger}$ is favorable for each dissociation process.

Electrostatic contribution to binding

Equilibrium binding experiments indicated that 11F8/**WT** complexation is accompanied by both cation and anion release.[9] The cation release is pH-dependent and results from the formation of salt bridges. To determine at which step this occurs, the binding experiments were repeated in buffers containing Cl^- and OAc^- anions. The slope of ln K_a versus ln [salt] is an indication of ion release as described by Record et al.[39] The effect of both salts were studied as anions are ranked by the Hoffmeister series,[40,41] according to their preferential exclusion from protein surfaces ($OAc^- \gg Cl^-$). If anion release occurs on binding, anions that have a lower affinity for protein surfaces (OAc^-) will have a smaller ion release than those that bind more strongly (Cl^-). During the formation of the 11F8/**WTAP** complex in NaCl buffers, three ions are released. The pre-equilibrium experiments indicate that two of these ions are released during the formation of the encounter complex and the third is released during the putative conformational change occurring in the second step. Only two ions are released when the complex forms in buffers containing NaOAc, both during the formation of the encounter complex. These data suggest that two cations are released during the first step of the interaction and an anion is released during the second step.

LS binding to 11F8 results in the same salt release stoichiometry as **WTAP** (Table 4). However, formation of the 11F8/**T7** complex is different. Both the kinetic and equilibrium data show that there is no apparent anion release. The pre-equilibrium data indicates that three cations are released upon binding to 11F8 in NaCl buffers, but that 1.5 ions are released in each step. This observation suggests that at least two different encounter complexes exist, one where two cations have been released and one where only one has been released. The presence of a multi-species encounter complex possibly results from the overlapping 'thymine binding sites' present on **T7** sequence.[6] Cation release during the second step could be a result of a conformational change as suggested by the lack of an observed pH dependence,[9] or through salt bridge formation. Interestingly, this effect is only seen in NaCl buffer and not in NaOAc buffer where two ions are released during step 1 and the third during step 2. This result may arise from differences in recognition due to changes in the anion bound to 11F8, or reflect differences in the water structure around the protein surface due to the presence of the acetate ion (Fig. 5).[40]

Table 3. (a) Activation energies for the association and dissociation of the 11F8/ssDNA complexes presented in kcal/mol; (b) enthalpies of activation calculated from the Eyring plot, $1/T$ versus $\ln(k/T)$ where the slope $= -\Delta H^{\ddagger}/R$ and given as kcal/mol; (c) entropies of activation for each binding step calculated from the Eyring plot described above where the y-intercept $= \ln(k_B/h) + \Delta S^{\ddagger}/R$ and presented in cal/mol/K

	Sequence	k_1	k_{-1}	k_2	k_{-2}
(a)	**WTAP**	5.3±0.3	14.3±1.4	8.9±0.9	31.5±1.5
	$T_{11}dU$	4.9±0.5	14.6±1.0	8.2±0.7	26.5±2.1
	LS	5.1±0.3	13.9±1.2	7.4±0.5	23.3±1.8
	T7[1]	4.4±0.3	12.3±1.4	10.3±0.6	20.4±1.6
(b)	**WTAP**	4.4±0.3	16.6±1.3	8.4±0.8	30.9±2.1
	$T_{11}dU$	3.7±0.3	15.9±1.8	7.5±0.4	21.3±1.7
	LS	3.8±0.2	16.3±1.2	6.2±0.7	17.8±1.1
	T7[1]	3.1±0.2	11.1±1.4	6.6±0.5	18.4±1.4
(c)	**WTAP**	−37.4±3.2	41.5±4.7	−12.61±1.3	74.1±5.6
	$T_{11}dU$	−36.4±6.4	44.6±5.1	−13.2±1.7	70.3±5.5
	LS	−40.3±5.1	53.2±7.2	−17.9±2.1	66.4±5.1
	T7[a]	−37.8±4.1	42.4±4.4	−22.4±2.4	51.3±3.7

[a]20 mM TrisHCl pH 8.0, 150 mM NaCl, 20% w/v sucrose.

Polarity experiments

The interaction of **WT**, **LS,** $T_{11}dU$ and **T7** with 11F8 is sensitive to bulk solvent polarity.[9] This sensitivity presumably results from hydrophobic interactions between

Table 4. Salt release stoichiometry for each step of the interaction

Sequence	$-SK_{a(eq)}$ (k_1/k_{-1})	$-SK_{a(eq)}$ (k_2/k_{-2})	$-SK$
WTAP (NaCl)	1.3±0.1	0.582±0.04	1.9±0.2
WTAP (NaOAc)	1.4±0.1	0.107±0.01	1.3±0.1
$T_{11}dU$ (NaCl)	1.3±0.2	0.642±0.02	2.0±0.1
$T_{11}dU$ (NaOAc)	1.4±0.1	0.0544±0.001	1.3±0.2
LS (NaCl)	1.5±0.2	0.713±0.04	2.5±0.2
LS (NaOAc)	1.5±0.2	0.091±0.03	1.6±0.2
T7 (NaCl)	1.0±0.2	0.98±0.2	2.2±0.1
T7(NaOAc)	1.4±0.1	0.682±0.05	2.1±0.2

non-polar surfaces of 11F8 and ssDNA bases (i.e., desolvation of the binding interface). Previous studies have shown that reducing the bulk solvent polarity decreases binding affinity.[9] The salt release stoichiometry data presented above suggest that the initial step of the interaction involves electrostatic interactions, the strength of which should increase in a decreasing polar environment. To examine whether the overall decrease in affinity observed at equilibrium is mediated through the second step of binding, we studied the effect of buffers containing methanol and 1-propanol on the kinetics of complex formation.

Upon the addition of either of these alcohols, the affinity of the encounter complex is increased which supports the data indicating that electrostatic interactions are important for complex stability. The importance of the dielectric constant for each step of binding and at equilibrium for the 11F8/**WTAP** complex is presented in Figure 6, the data measured using the individual solvents for each sequence are in Table 5. A large decrease in affinity is observed for the second step which is mediated through changes in both k_2 and k_{-2} contributes to the overall decrease in affinity observed at equilibrium. The decrease in affinity in step 2 is larger than that observed at equilibrium compensating for the increase in affinity of the encounter complex. This decrease probably arises because the interaction of the solvents with the non-polar surfaces on 11F8 and/or **WTAP** are favorable relative to that between the non-polar surfaces on 11F8 and **WTAP**.

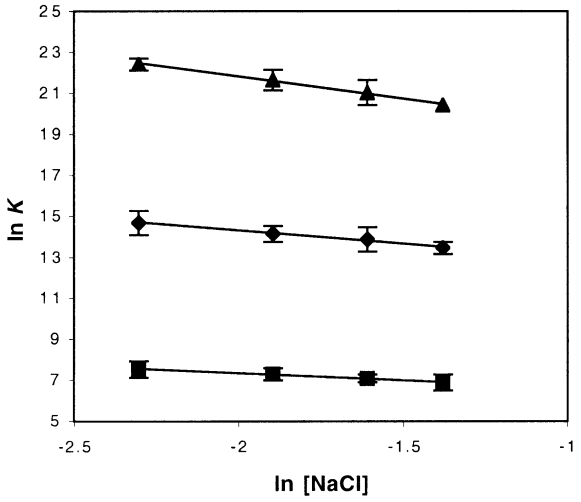

Figure 5. Dependence on the affinity of each binding step in the 11F8/**WT** complex on [NaCl]. The data shown is the relationship if k_1/k_{-1} (◆), k_2/k_{-2}(■) and $K_{a(eq)}$ (▲).

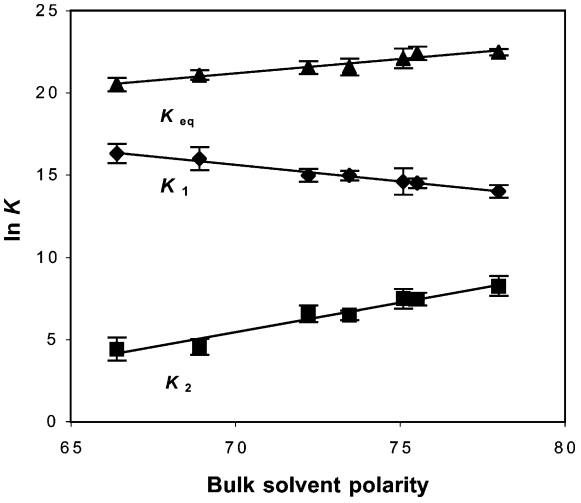

Figure 6. Dependence on each step of the 11F8/**WT** interaction on bulk solvent polarity. k_1/k_{-1} (◆) shows an increase in affinity in the decreasing polar environment, while k_2/k_{-2} (■) and $K_{a(eq)}$ (▲) indicate a decrease in affinity for the decreasing polarity. This data includes the affinities measured in both methanol and 1-propanol buffers. As the ratio of the association and dissociation rates is studied, any changes in viscosity due to the addition of the solvents cancel.

Discussion

Previous binding-site selection experiments performed with a panel of clonally related autoantibodies isolated from a lupus-prone mouse demonstrated that 11F8 is sequence specific.[8] The specific sequence (**WT**) possesses a -GYYTTC- recognition epitope within the context of a hairpin structure containing a four-base loop (C_8–T_{11}) separated from a single-base bulge by three base-pairs. A comprehensive binding study carried out under equilibrium conditions identified that both sequence and structure are required for high affinity complex formation with **WT**.[9] The interaction of 11F8 with **WT** and noncognate ligands is characterized by a favorable enthalpy, an unfavorable entropy, and little dependence on the polyelectrolyte effect. In addition, recognition of **WT** is accompanied by a negative change in heat capacity. The interaction with **NS**, however, is completely entropically driven ($\Delta H = 0$), characteristic of true nonspecific recognition.[42]

The nature of step 1

The pre-equilibrium experiments described here reveal that sequence-specific, noncognate, and nonspecific recognition occurs in two steps. An initial association is observed leading to the formation of an encounter complex with dissociation constants in the micromolar range. The initial k_{obs} measured for the interaction with each ligand is fast, and is accompanied by a small fluorescence change. To investigate the first step, sucrose

Table 5. Dependence of each binding step on the bulk solvent polarity

Sequence	Solvent	S (k_1/k_{-1})	S (k_2/k_{-2})	$SK_{a(eq)}$
WT	Methanol	−0.10±0.02	0.33±0.02	0.17±0.01
	1-Propanol	−0.14±0.01	0.35±0.03	0.18±0.02
T_{11}dU	Methanol	−0.13±0.02	0.3±0.01	0.18±0.02
	1-Propanol	−0.15±0.02	0.34±0.02	0.19±0.03
LS	Methanol	−0.11±0.01	0.28±0.02	0.18±0.01
	1-Propanol	−0.12±0.01	0.32±0.03	0.21±0.02
T7	Methanol	−0.15±0.02	0.34±0.02	0.17±0.01
	1-Propanol	−0.17±0.01	0.38±0.03	0.20±0.01

was added to the binding buffer to slow the rate at which the molecules interact. Due to the wide range of k_{obs} measured, the same experimental conditions could not be used for each DNA ligand, consequently direct comparisons of the data cannot be made. However, assuming that the dependence of each rate is linear over the range of conditions studied ([salt], [sucrose], and temperature), each rate can be extrapolated to reach common solution conditions. We chose 20 mM Tris–HCl, 150 mM NaCl at 25 °C as a reference point (Table 6) since other protein/protein[29,30,43] and protein/nucleic acid[10,13,17] binding mechanisms have been determined under similar conditions.

The values of k_1 and k_{-1} are similar for the binding of 11F8 to **WT**, T_{11}dU and **LS** indicating that the observed specificity for these ligands is not determined during the initial step. However, the 11F8/**T7** complex forms more quickly (6-fold) indicating that processes leading to the encounter complex, are not the same as for the other ligands. This difference may reflect the overlapping binding sites present within **T7**, or a decrease in the specificity in the initial complex. Polarity and salt studies show that ionic interactions participate in the initial binding step of **WT**, T_{11}dU and **LS** with 11F8, and the salt release stoichiometry suggests that two electrostatic contacts are formed. The rate of k_1 for these ligands is higher than the modified Smoluchowski limit for the estimated rate at which diffusion restricts the initial collision (10^5–10^6 M^{-1} s^{-1}).[43,44] An association rate that exceeds this estimate is common for both protein/protein and protein/nucleic acid interactions and is often attributed to electrostatic steering.[29,36,43,44] This phenomenon requires that two interacting molecules have opposite surface charges, the attraction of which allows them to position themselves into approximately the correct binding orientation prior to any initial collision, thus increasing the probability of a successful interaction. Once the initial contact has been made, a complex can undergo a series of mini-collisions that allows the stabilizing salt bridges to be made.[36,45] Within the CDR loops of 11F8, there are seven positively charged residues (both arginine and lysine) that could attract the negative phosphate groups of ssDNA ligands.[24,46]

Step 2 determines specificity between 11F8 and the specific and noncognate sequences

If the initial steps in 11F8 recognition of **WT**, **LS** and T_{11}dU are virtually the same, specificity must be governed by the second binding step. This two step mechanism has been observed in other in biological systems and the second step is frequently a conformational change.[29,42] No change in molar ellipiticity was observed when complex formation was examined by CD,[9] indicating that no significant change in secondary structure occurs within either 11F8 or DNA ligands upon binding. However, in some protein/protein complexes, including those between antibodies and antigens, these conformational changes are small, often involving alterations in backbone conformation and side-chain orientation[31,47,48] that are not detectable in far UV CD experiments. Hence, conformational changes that may occur within 11F8, DNA, or both, could be small and outside the detection limits of CD.

Table 6. Estimated kinetic parameters for each step of the interaction in 20 mM Tris–HCl, 150 mM NaCl, pH 8.0 at 25 °C (assuming that the temperature coefficient for each step is linear over this temperature range)

Sequence	k_1 (M^{-1} s^{-1})	k_{-1} (s^{-1})	k_2 (s^{-1})	k_{-2} (s^{-1})
WT	6.2×10^7	36	5.1	0.0095
T_{11}dU	6.0×10^7	38	5.0	0.048
LS	7.1×10^7	47	4.8	0.065
T7	3.8×10^8	185	3.4	0.106
NS	9.0×10^8	305	ND	ND

Less than a 2-fold difference is observed between the values of k_2 for each of the ssDNA ligands indicating that the second (forward) step does not directly account for the difference in affinity. In contrast the values of k_{-2} for binding **WT** and the noncognate ligands vary up to 160-fold indicating that specificity is predominantly mediated through the dissociation of the final complexes as observed in other specific protein/protein and protein/DNA complexes.[42,49,50] The second step of the interaction of 11F8 with either **WT** or noncognate sequences is driven by the desolvation (k_2)/hydration (k_{-2}) of hydrophobic surfaces within the binding site. Desolvation is a prerequisite for base stacking interactions which are commonly observed within protein/ssDNA complexes[51,53] including the anti-ssDNA autoantibody, BV04-01 bound to dT_3.[52,54]

Previous footprinting studies of the 11F8/**WT** complex show that T_{10} and T_{11} are buried within the complex, consistent with base stacking interactions.[8,9] Protection of the thymine bases within the 11F8/T_{11}dU and 11F8/**LS** complexes indicate that these bases are also buried within the binding site and thus may be stacking in spite of the decreased affinity. Changes in the DNA sequence or structure of the specific recognition site can effect the hydration shell, altering the desolvation process, and affecting the affinity of these complexes.[9] However, no appreciable difference in the effect of bulk solvent polarity on the second step for the specific and noncognate complexes is observed (Table 5). This finding indicates that either the polarity experiments are not sensitive enough to distinguish small differences in the desolvation processes, and/or that once the hydrophobic surfaces are buried within the binding site, additional contacts, such as hydrogen bonds are formed that increase the affinity of 11F8/**WT** complex.

Nonspecific recognition

The formation of the 11F8/**NS,** encounter complex does not follow the same association pathway as the other sequences. Equilibrium experiments revealed that binding of **NS** is entropically driven accompanied by the formation of up to 10 salt bridges.[9] The value of k_1 is 10-fold greater than k_1 for the 11F8/**WT** complex, however, as the net negative charge of the DNA is not greater than the other sequences this increased rate

cannot result from electrostatic steering effects. This observation suggests that the encounter complexes formed by the other sequences are different from that formed with **NS**. As there are no sequence constraints to influence the interaction between **NS** and 11F8, the location of the initial contacts formed by the molecules can occur randomly along the DNA resulting in a number of different encounter complex species. The multi-phase reaction trace and the difference between affinity of the pre-equilibrium and equilibrium complexes suggest that at least one additional step occurs after the encounter complex is formed, during which binding is optimized. However, the rate of this step will be determined by the conformation of the particular encounter complex. Consequently, with a series of alternative complexes in solution, each subsequent step will be described by a different rate, resulting in the complex reaction kinetics observed.

Conclusion

The specificity of 11F8 for **WT** and noncognate ligands relative to **NS** is governed in part by interactions formed during the encounter complex. This initial complex is stabilized through the formation of electrostatic interactions. Additional stability is gained through the second, rate-limiting step, during which small structural changes may occur that increase the complementarity of the binding surface allowing additional contacts to form. This step is driven by the desolvation at the binding interfaces. The kinetic basis behind the specificity of 11F8 lies in the dissociation of the complexes, which reflects the strength of the contacts formed during the second step of the interaction. The data are consistent with the induced fit mode for antibody/antigen binding,[48,55] where small conformational changes occur upon complexation that maximize favorable interactions, and demonstrates the prominent role of solvent on macromolecular recognition processes.

Material and Methods

Materials

Reagents for the buffers were Beacon® Ultralow fluorescence grade, purchased from Panvera, Madison, WI. Additional chemicals were obtained from Sigma (St Louis, MO) and Fischer Scientific (Pittsburgh, PA).

11F8 and DNA preparation

The preparation of mAb 11F8 and DNA sequences has been described elsewhere.[6–9] Both the protein and DNA were >98% pure, judged from polyacrylamide gel electrophoresis and HPLC.

Steady state fluorescence measurements

All steady state fluorescence measurements were carried out using a Spectronic AB2 fluorimeter equipped with a magnetic stirrer. The temperature was maintained with a thermostated cellblock regulated by a Neslab circulating water bath. For measuring binding isotherms, the excitation and emission wavelengths were set at 280 and 336 nm for tryptophan fluorescence, and 310 and 360 nm for 2AP fluorescence. The slit widths were set at 4 and 8 nm for excitation and emission wavelengths, respectively. Data were collected over a 15 s period allowing 30 s after the addition of each aliquot of DNA for equilibration to occur. The absorbance of all samples was measured at the appropriate excitation and emission wavelengths and corrections were made for the inner filter effect when OD >0.05 based on the following equation:

$$F_{corr} = F_{obs}\ \exp(0.5A_{ex} + 0.5A_{em}) \quad (2)$$

where F_{corr} and F_{obs} are the fluorescence values for the corrected and observed emission, respectively, and A_{ex} and A_{em} are the absorbance values at the excitation and emission wavelengths. The analysis of the binding isotherms has been described fully elsewhere.[9]

Stopped-flow measurements

Stopped-flow measurements were conducted using π*-CDF or SX.18MV stopped-flow spectrophotometers from Applied Photophysics Ltd (Surrey, UK). Both machines were fitted with 2 mL syringes to give a mixing ratio of 1:1 v/v. The slitwidths for both the excitation and emission light were set at 1.5 nm. Measurements were made over a range of time periods collecting 1000 data points. Excitation wavelengths were the same as those for the equilibrium measurements, and emission of the individual fluorescent groups was monitored by use of suitable cut off filters. All measurements were carried out in 20 mM Tris–HCl, pH 8.0, 150 mM NaCl, 10% w/v sucrose at 5 °C unless otherwise stated. Each measurement was carried out at least five times, analyzed individually, and as an average by single or double exponential curve fitting algorithms using the software supplied by the manufacturer. The single exponential analysis employed is described in eq (3):

$$F_t = F_0\exp(-kt) + C \quad (3)$$

where F_0 and F_t are the fluorescence intensities at time 0 and time t, respectively, k is the apparent first-order rate constant for the reaction, and C is a constant. Double exponential analysis was carried out using eq (4):

$$F(t) = A_1\exp(-k_1t) + A_2\exp(-k_2t) + C \quad (4)$$

where $F(t)$ is the fluorescence at time t, A_1 and A_2 are the amplitudes of the different phases and k_1 and k_2 are the rates of the first and second phases, respectively, and C is a constant.

In experiments to determine the association rates for complex formation, [11F8] = 100 nM (all concentrations are before mixing) while the DNA kept in constant excess of [11F8] (10- to 15-fold). Thus, pseudo-first order reaction conditions were approached and from plots of [DNA] versus k_{obs}, the apparent second-order

rate constants k_{on} were calculated from the slopes, and values of k_{off} were obtained from the y-intercepts.

Dissociation experiments of the 11F8/**WTAP** (**WT** containing 2AP in place of G_4) and 11F8/T_{11}dU complexes were performed by mixing a solution (1:1 v/v) containing 11F8 (100 nM) and **WTAP** (200 nM) that had been equilibrated for 1 h, with an excess of **WT** (2 μM). The fluorescence of 2AP was monitored as the complex dissociated. The 2AP within the **T7** and **LS** sequences gave no change in emission on complexation with 11F8, so the rate of dissociation was measured by mixing the preformed complexes with an excess of **WTAP** and monitoring the change in 2AP of **WTAP** as it binds to the newly dissociated 11F8.

Analysis of the temperature dependence of the association and dissociation rate constants

The equilibrium and pre-equilibrium experiments were repeated over the temperature range of 3–11 °C. The activation energy (E_a) for each step was determined from the Arrhenius equation;

$$k = Ae^{-E_a/RT} \quad (5)$$

where k is the rate constant. The slope of the plot $1/T$ versus ln k gives $-E_a/RT$. The enthalpy and entropy of activation for each step was determined using the Eyring equation;

$$k = (k_B T\kappa/h)\ e^{(\Delta S^{\ddagger}/R)}\ e^{-(\Delta H^{\ddagger}/RT)} \quad (6)$$

where k is the rate constant, k_B is Boltzman constant, κ is the transmission constant (taken as 1),[38] h is Plancks constant and $\Delta H^{\ddagger}$ and $\Delta S^{\ddagger}$ are the enthalpy and entropy of activation, respectively. The plot of $1/T$ versus ln (k/T) has a slope of $-\Delta H^{\ddagger}/RT$ and a y-intercept of ln $(k_B/h) + \Delta S^{\ddagger}/R$.

The change in viscosity of the various buffers at different temperatures was determined using a falling ball viscometer (Gilmont Instruments, IL).[56,57] The results were fitted to a polynomial equation. The subsequent data were corrected to give the k_{obs} expected for the viscosity observed in the buffer in use (i.e., 10 or 20% w/v sucrose) at 5 °C.

Polarity experiments

The effect of changing solvent polarity was measured by repeating the association and dissociation experiments in buffers which contained different amounts methanol and 1-propanol. The dielectric constants of the aqueous solutions were calculated from empirical relationships based upon weight percent.[58]

Acknowledgements

This work was supported by NIH grant GM 46831.

References and Notes

1. Tan, E. M. *Adv. Immunol.* **1989**, *44*, 93.
2. Koffler, D.; Schur, P. H.; Kunkel, H. G. *J. Exp. Med.* **1967**, *126*, 607.
3. Waer, M. *Clin. Rheumatol.* **1990**, *9*, 111.
4. Isenberg, D. A.; Ehrenstein, M. R.; Longhurst, C.; Kalsi, J. K. *Arthritis Rheum.* **1994**, *37*, 169.
5. Ben-Chetrit, E.; Eilat, D.; Ben-Sasson, S. A. *Immunol.* **1988**, *65*, 479.
6. Swanson, P. C.; Ackroyd, C.; Glick, G. D. *Biochemistry* **1996**, *35*, 1624.
7. Swanson, P. C.; Yung, R. L.; Blatt, N. B.; Eagon, M. A.; Norris, J. M.; Richardson, B. C.; Johnson, K. J.; Glick, G. D. *J. Clin. Invest.* **1996**, *97*, 1748.
8. Stevens, S. Y.; Glick, G. D. *Biochemistry* **1999**, *38*, 560.
9. Ackroyd, P. C.; Cleary, J.; Glick, G. D. *Biochemistry* **2001**, *40*, 2911.
10. Metzger, A. U.; Bayer, P.; Willbold, D.; Hoffmann, S.; Frank, R. W.; Goody, R. S.; Rosch, P. *Biochem. Biophys. Res. Com.* **1997**, *241*, 31.
11. Sha, M.; Ferre-D'Amare, A. R.; Burley, S. K.; Goss, D. J. *J. Biol. Chem.* **1995**, *270*, 19325.
12. Johnson, R. S.; Chester, R. E. *J. Mol. Biol.* **1998**, *283*, 353.
13. Parkhurst, K. M.; Richards, R. M.; Brenowitz, M.; Parkhurst, L. J. *J. Mol. Biol.* **1999**, *289*, 1327.
14. Barbas, S. M.; Ditzel, H. J.; Salonen, E. M.; Yang, W.-P.; Silverman, G. J.; Burton, D. R. *Proc. Natl. Acad. Sci., U.S.A.* **1995**, *92*, 2529.
15. Neylon, C.; Brown, S. E.; Kralicek, A. V.; Miles, C. S.; Love, C. A.; Dixon, N. E. *Biochemistry* **2000**, *39*, 11989.
16. LeBlanc, J. F.; McLane, K. E.; Parren, P. W. H. I.; Burton, D. R.; Ghazal, P. *Biochemistry* **1998**, *37*, 6015.
17. Hart, D. J.; Speight, R. E.; Cooper, M. A.; Sutherland, J. D.; Blackburn, J. M. *Nucleic Acids Res.* **1999**, *27*, 1063.
18. Jamieson, E. R.; Jacobson, M. P.; Barnes, C. M.; Chow, C. S.; Lippard, S. J. *J. Biol. Chem.* **1999**, *274*, 12346.
19. Toulme, J.-J.; Helene, C. *J. Biol. Chem.* **1977**, *252*, 244.
20. Jia, Y.; Kumar, A.; Patel, S. S. *J. Biol. Chem.* **1996**, *271*, 30451.
21. Oda, M.; Furukawa, K.; Sarai, A.; Nakamura, H. *FEBS Lett.* **1999**, *454*, 288.
22. Zhong, X.; Patel, S. S.; Werneberg, B. G.; Tsai, M.-D. *Biochemistry* **1997**, *36*, 11891.
23. Stivers, J. T.; Pankiewicz, K. W.; Watanabe, K. A. *Biochemistry* **1999**, *38*, 952.
24. Nadassy, K.; Wodak, S. J.; Janin, J. *Biochemistry* **1999**, *38*, 1999.
25. Urbanke, C.; Schaper, A. *Biochemistry* **1990**, *29*, 1744.
26. Joshi, R. V.; Zarutskie, J. A.; Stern, L. J. *Biochemistry* **2000**, *39*, 3751.
27. Gutfreund, H. *Kinetics for the Life Sciences*; Cambridge University: Cambridge, 2000.
28. Gore, M. G.; Bottomley, S. P. In *Spectrophotometry and Spectrofluorimetry*; Gore, M. G., Ed.; Oxford University: Oxford, 2000; pp 241–264.
29. Janin, J. *Proteins* **1997**, *28*, 153.
30. Wallis, R.; Moore, G. R.; James, R.; Kleanthous, C. *Biochemistry* **1995**, *34*, 13743.
31. Beckingham, J. A.; Bottomley, S. P.; Hinton, R.; Sutton, B. J.; Gore, M. G. *Biochem. J.* **1999**, *340*, 193.
32. Martin, G. E. M.; Rutherford, N. G.; Henderson, P. J. F.; Walmsley, A. R. *Biochem. J.* **1995**, *308*, 261.
33. Chaiyen, P.; Brissette, P.; Ballou, D. P.; Massey, V. *Biochemistry* **1997**, *36*, 2612.
34. Friguet, B.; Djavadi-Ohaniance, L.; Goldberg, M. E. *Res. Immunol.* **1989**, *140*, 355.
35. Foote, J.; Milstein, C. *Proc. Natl. Acad. Sci. U.S.A.* **1994**, *91*, 10370.

36. Camacho, C. J.; Weng, Z.; Vajda, S.; DeLisi, C. *Biophys. J.* **1999**, *76*, 1166.
37. Anderson, T. G.; McConnell, H. M. *Biophys. J.* **1999**, *77*, 2451.
38. Jencks, W. P. *Catalysis in Chemistry and Enzymology*; McGraw-Hill: New York, 1969.
39. Record, M. T. J.; Lohman, T. M.; deHaseth, P. L. *J. Mol. Biol.* **1976**, *107*, 145.
40. Collins, K. D.; Washabaugh, M. W. *Q. Rev. Biophys* **1985**, *18*, 323.
41. Cacace, M. G.; Landau, E. M.; Ramsden, J. J. *Q. Rev. Biophys* **1997**, *30*, 241.
42. Oda, M.; Nakamura, H. *Genes to Cells* **2000**, *5*, 319.
43. Schreiber, G.; Fersht, A. R. *Nat. Struct. Biol.* **1996**, *3*, 427.
44. Selzer, T.; Schreiber, G. *J. Mol. Biol.* **1999**, *287*, 409.
45. Wade, R. C.; Gabdoulline, R. R.; Ludemann, S. K.; Lounas, V. *Proc. Natl. Acad. Sci. U.S.A.* **1998**, *95*, 5942.
46. Blatt, N. B.; Bill, R. M.; Glick, G. D. *Hybridoma* **1998**, *17*, 33.
47. Kondo, H.; Shiroishi, M.; Matsushima, M.; Tsumoto, K.; Kumagai, I. *J. Biol. Chem.* **1999**, *274*, 27623.
48. Davies, D. R.; Sheriff, S.; Padlan, E. A. *J. Biol. Chem.* **1988**, *263*, 10541.
49. Selzer, T.; Albeck, S.; Schreiber, G. *Nat. Struct. Biol.* **2000**, *7*, 537.
50. Wallis, R.; Leung, K.-Y.; Pommer, A. J.; Videler, H.; Moore, G. R.; James, R.; Kleanthous, C. *Biochemistry* **1995**, *34*, 13751.
51. Raghunathan, S.; Kozlov, A. G.; Lohman, T. M.; Waksman, G. *Nat. Struct. Biol.* **2000**, *7*, 648.
52. Herron, J. N.; He, X. M.; Ballard, D. W.; Blier, P. R.; Pace, P. E.; Bothwell, A. L. M.; Voss, E. W., Jr.; Edmundson, A. B. *Proteins* **1991**, *11*, 159.
53. Shamoo, Y.; Friedman, A. M.; Parsons, M. R.; Konigsberg, W. H.; Steitz, T. A. *Nature* **1995**, *376*, 362.
54. Swanson, P. C.; Cooper, B. C.; Glick, G. D. *J. Immunol.* **1994**, *152*, 2601.
55. Wirsching, P.; Ashley, J. A.; Benkovic, S. J.; Janda, K.; Lerner, R. A. *Science* **1991**, *252*, 680.
56. Muller, F. J.; Pita, J. C. *Anal. Biochem.* **1983**, *135*, 106.
57. Campbell, D.; White, J. R. *Polmer Characterization*; Chapman and Hall: London, 1989.
58. Akerlof, G. *J. Am. Chem. Soc.* **1932**, *54*, 4125.